

Contents lists available at [ScienceDirect](http://ScienceDirect.com)

# Algal Research

journal homepage: [www.elsevier.com/locate/algal](http://www.elsevier.com/locate/algal)

## Production of bio-coal, bio-methane and fertilizer from seaweed via hydrothermal carbonisation



Aidan M. Smith, Andrew B. Ross\*

School of Chemical and Process Engineering, University of Leeds, Leeds, UK

### ARTICLE INFO

#### Article history:

Received 19 September 2015

Received in revised form 23 February 2016

Accepted 26 February 2016

Available online 5 March 2016

#### Keywords:

Macroalgae

Hydrothermal carbonisation

Hydrochar

Anaerobic digestion

Nutrients

### ABSTRACT

Macroalgae have emerged as a potential future source of feedstock for the production of chemicals and biofuels. The main drawbacks of macroalgae in terms of a biofuel feedstock are its low heating value (HHV), high halogen content, high ash content and high slagging and fouling propensity. In this investigation, three species of kelps; (i) *Laminaria digitata* (ii) *Laminaria hyperborea* and (iii) *Alaria esculenta* have been processed by hydrothermal carbonisation (HTC) in a batch reactor at two temperatures (200 °C and 250 °C). The yields and properties of the resulting hydrochars including their HHV, CHNS, mineral content and ash fusibility properties have been determined and compared to the starting material. Significant improvement in fuel quality is observed resulting in an increase in energy density from 10 MJ/kg to typically 25 MJ/kg, which is comparable to that of a low rank coal. The results indicate significant demineralisation of the fuel, in particular a significant removal of alkali salts and chlorine. This results in improved combustion properties due to a reduction in the slagging and fouling properties of the fuel. Analysis of the HTC water phase indicates the presence of high levels of soluble organic carbon consisting of sugars and organic acids, and high levels of potassium, magnesium and phosphorous. The potential for production of bio-methane and recovery of nutrients following anaerobic treatment of the water phase is assessed. A prediction of the bio-methane yields for the different seaweeds has been calculated. Processing of biomass collected throughout the growth season indicates the influence of seasonal variation on energy and nutrient recovery.

© 2016 The Authors. Published by Elsevier B.V. This is an open access article under the CC BY license (<http://creativecommons.org/licenses/by/4.0/>).

### 1. Introduction

Biofuels derived from aquatic biomass such as macroalgae offer an extensive and largely unutilised biomass resource which do not compete with agriculture or forestry for land and freshwater; overcoming drawbacks associated with using terrestrial biomass to produce biofuels. Macroalgae have several advantages over terrestrial biomass and include high growth rates due to their high photosynthetic activity and reduced land requirements [15]. Macroalgae can be divided into three categories: (i) brown algae (phaeophyceae); red algae (rhodophyceae); and green algae (chlorophyceae) and have been used as an industrial feedstock throughout history [36]. Macroalgae is an industrially valuable and versatile commodity, producing foods, cosmetics and fertilizers from phycocolloids and alginates. Brown algae typically yield 15–20 dry tonnes per hectare per year and there is a growing interest in Europe in the cultivation and farming of seaweed for energy [36].

Although macroalgae offer a potentially large biomass resource, they are significantly different from terrestrial plants in terms of their

chemical composition [26]. They do not contain high levels of lignocellulose and are instead predominantly comprised of carbohydrate in the form of mannitol, laminarin, fucoidan, alginic acid and other polysaccharides [35]. To give the algae support in the absence of lignin, brown algae use parallel chains of polymeric alginic acid bound by alkali and alkaline metals [21]. Consequently brown algae accumulate alkali and alkaline earth metal ions, notably  $K^+$ ,  $Na^+$  and  $Ca^{2+}$ , which are found in concentrations in the order of  $10^4$  ppm, giving high ash contents [2]. An additional significant proportion of these cations can be associated with halogens such as KCl. The remaining organic fraction includes protein and fucoidan which results in comparatively high levels of nitrogen and sulphur respectively [35].

Macroalgae are generally high in chlorine, high in ash, have low calorific value and high moisture content [35]. While the exact chemical compositions of macroalgae vary between species, there is additional compositional variation within single species, both seasonally and geographically [10] and the impact of this will influence the energy content throughout the year. Studies of the seasonal variation of seaweed composition have been reported for a number of UK brown seaweeds and generally show that the carbohydrates such as laminarin and mannitol peak in the summer resulting in the highest energy content. In contrast,

\* Corresponding author.

E-mail address: [a.b.ross@leeds.ac.uk](mailto:a.b.ross@leeds.ac.uk) (A.B. Ross).

the protein, ash and alginic acid content peak in the winter months resulting in lower calorific values [2,37]. Harvesting toward the end of September results in a feedstock with the highest carbon content and the lowest nitrogen content [37].

This significant compositional difference between terrestrial biomass and macroalgae means that 'conventional' biomass treatments are less suitable. The high chlorine, ash and alkali content, low calorific value and high moisture content make macroalgae an unattractive option for combustion, pyrolysis or gasification without some form of pre-treatment due to the energy requirements in thermal drying and unfavourable ash chemistry resulting in slagging, fouling and corrosion [35]. As a consequence, the majority of research into utilising macroalgae as a biofuel has focused on the production of biogas by anaerobic digestion (AD) [1,17,23] or the production of bio-ethanol via fermentation [22,26]. Investigations into the pre-treatment of macroalgae have been principally focused on reducing the levels of metals using acid washing. Up to 90% reduction in Mg, K, Na, and Ca ions has been reported along with a reduction in nitrogen and halogens [7,34]. This pre-treatment could make combustion, pyrolysis or gasification more attractive although the acid washing also leads to the partial removal of laminarin, fucoidan and mannitol leading to the dominance of alginic acid in the fuel [34].

An additional thermochemical route under investigation is called hydrothermal processing. This is the collective term for three different processes: hydrothermal carbonisation (HTC), hydrothermal liquefaction (HTL) and hydrothermal gasification (HTG) and involves the processing of biomass in compressed water at elevated temperature. Hydrothermal processing is more tolerant to high moisture and ash containing feedstocks such as macroalgae. To date, most research into the hydrothermal processing of macroalgae has focused on hydrothermal liquefaction to produce oils and supercritical water gasification to produce syngas [5,12]. There has been only limited investigation of the hydrothermal carbonisation of macroalgae. Hydrothermal carbonisation operates at temperatures between 180 and 250 °C with the main product being a solid char-like residue exhibiting similar properties to that of a low rank coal known as a bio-coal or hydrochar. The coal like bio-coal is: (i) more energy dense, (ii) more easily friable and (iii) more hydrophobic than the starting material. Until recently only Xu et al. [42] have published on the HTC of macroalgae with the aim to produce an energy carrier while others have investigated the production of organic chemicals [25] and carbon microspheres [11] via hydrothermal processing of alginate. The authors have investigated the fate of ash during HTC of a range of biomass including macroalgae. The results indicate a significant increase in carbon content in the resulting bio-coal along with a significant reduction in oxygen content resulting in increased energy densification. Analysis of the ash indicated a significant removal of the alkali metals, K and Na, with more limited removal of Mg and Ca [39]. Analysis of the ash behaviour during combustion of the bio-coal indicated that HTC reduces the slagging propensity of the resulting bio-coal. The results were significant as the HTC process appears to overcome the physiochemical problems associated with macroalgae which prevent its utilisation in combustion, pyrolysis or gasification, producing a bio-coal, with a similar calorific value to a low rank coal with much improved combustion properties [39].

Despite the main product being the bio-coal, the other products include a process water phase containing polar organic compounds and mineral matter and a gaseous fraction mostly comprised of CO<sub>2</sub>. Anaerobic treatment of the aqueous phase following HTC of biomass has been suggested as a potential route to optimise energy recovery [41]. The degradation of complex organic matter during the HTC process to organic acids, particularly formic acid and acetic acid, should enable relatively fast degradation, providing the absence of inhibition [41]. Wirth and Mumme [41] have also demonstrated the biological methane production (BMP) of process water from corn silage to be in the region of 0.5–1 l methane per g of TOC (total organic carbon). The BMP of the

process waters can be predicted by using the Buswell or Boyle's equation if the carbon, hydrogen, nitrogen and oxygen content of the process water is known [13].

This investigation sets out to investigate the feasibility of using HTC to produce a high quality solid fuel which could be used in both domestic and commercial furnaces. The investigation looks at three species of UK indigenous brown kelp; (i) *Laminaria digitata* (ii) *Laminaria hyperborea* and (iii) *Alaria esculenta*. The investigation assesses how the seasonal compositional variation of the seaweed affects the solid fuel quality and calculates the potential for energy recovery by anaerobic treatment of the process waters. In addition, the potential for recovery of key plant nutrients such as potassium, phosphorous and ammonia is discussed.

## 2. Methodology

### 2.1. Materials

Samples of macroalgae were provided by the Scottish Association for Marine Science (SAMS) in Oban. Three species of macroalgae; (i) *L. digitata* (ii) *L. hyperborea* and (iii) *A. esculenta*, were harvested from wild kelp beds at Easdale on the west coast of Scotland in July for each species. In addition, samples of *L. hyperborea* were also collected at 4 intervals in the growth cycle including the spring (April), autumn (October) and winter (January) at the same location to assess the influence of seasonal compositional variation of seaweed on the biofuel quality. Samples under investigation were weighed upon collection (wet weight) and subsequently weighed after freeze drying (dry weight) by SAMS. The resultant dry weight of the freshly harvested samples was found to range between 11 and 20 wt.%. This is consistent with early work by Black [10] who found the seasonal variation in dry weight to be between 11 and 22.5 wt.%.

### 2.2. Hydrothermal carbonisation

HTC was performed in a 600 ml Parr batch reactor (Parr, USA) at 200 °C and 250 °C at their isobaric pressures of 16 bar and 40 bar respectfully. The temperature of the reactor was controlled by a PID controller. For each run, 24 g of freeze dried sample and 220 ml of distilled water were loaded into the reactor giving a solid loading of 10%. The macroalgae used in HTC were processed as received (unground) and were simply rehydrated when mixed with the distilled water. The reactor was weighed and then heated to the desired temperature at approximately 8 °C minute<sup>-1</sup> and the reaction temperature held for 1 h. After 1 h the reactor was allowed to air cool to room temperature (approximately 2 1/2 h from 200 °C; 3 h from 250 °C). When cooled, the reactor was depressurised into a gas sampling bag for gas analysis and the reactor reweighed to calculate gas and moisture loss along with the remaining combined mass of process water and bio-coal. The solid and liquid products were separated by filtration under vacuum using 110 mm qualitative circles (Grade 15, Munktell, UK). The process water was then stored and the reactor and char rinsed with a known volume of distilled water to recover any remaining sample. The bio-coal was allowed to air dry in a ventilated fume cupboard for a minimum of 48 h. Mass of the recovered process water was calculated by subtracting the dry mass of bio-coal from the combined mass of process water and bio-coal.

### 2.3. Analysis

#### 2.3.1. Inorganic analysis

The bio-coal and raw biomass to be used for analytical purposes were air dried and homogenised in a Retsch grinder. To determine the inorganic elemental composition (excluding silicon) samples were microwave digested (Aston Parr, USA) with 200 mg of sample in 10 ml concentrated nitric acid (HNO<sub>3</sub>). Potassium, sodium, calcium,

magnesium and iron were determined by AAS (Valiant, USA), phosphorus and silicon determined using colorimetry based methods and heavy metals determined by ICP-MS (Perkin Elmer, USA). The AAS and colorimetric methods were calibrated using standard elemental stock solution (Spectrosol, UK) and two certified biomass reference materials (Elemental Microanalysis, UK) were used to check the calibration and extraction efficiency.

Phosphorus was determined by reacting the acid digested sample with ammonium molybdovanadate solution (0.625 g ammonium metavanadate in 200 ml in 1:1 nitric acid added to 25 g of ammonium molybdate in 200 ml of deionised water and made up to 500 ml). The colour change was allowed to develop for 30 min and measured at 430 nm in a UV-visible photospectrometer (Thermo Scientific, USA). The silicon content was determined by ashing the biomass and bio-coal samples overnight in a muffle furnace then dissolving 50 mg of ash in a sodium hydroxide melt (1.5 g NaOH). Once cooled, 25 ml of distilled water was added and the sample heated on a steam bath for 30 min, the sample was then decanted and thoroughly rinsed into a 600 ml glass beaker and the solution made up to approximately 400 ml with distilled water. 20 ml of 1:1 hydrochloric acid (HCL) is then added and the solution decanted and rinsed into a 1000 ml volumetric flask which is made up to volume using distilled water. 10 ml of solution was then transferred into a 100 ml volumetric flask, diluted to 50–60 ml with distilled water and 1.5 ml of ammonium molybdate solution was added (7.5 g ammonium molybdate, in 75 ml distilled water, followed by 10 ml 1:1 sulphuric acid and finally made up to 100 ml). The solution was allowed to stand for 10 min before 4 ml of tartaric acid solution added (10 g tartaric acid in 100 ml distilled water), followed immediately by 1 ml reducing solution (20 ml 45% sodium hydrogen sulphite solution in 90 ml water, mixed with 0.7 g sodium sulphate and 0.15 g 4-amino 3-hydroxynaphthalene 1-sulphonic acid dissolved in 10 ml distilled water). Solutions were allowed to develop for 1 h and the concentration of silicon determined by absorbance at 650 nm in a UV-visible photospectrometer (Thermo Scientific, USA). Titanium dioxide content was determined by adding 5 ml of 1:1 sulphuric acid to 50 ml of acid digested sample followed by 5 ml hydrogen peroxide and measuring the 410 nm (Thermo Scientific, USA). Calibration solutions were made using standard elemental stock solution (Spectrosol, UK).

Chlorine within the feedstock and bio-coal was analysed by combustion in an oxygen bomb (Parr, USA) and an aqueous absorption media. Chlorine content was then measured by ion exchange chromatography (Dionex, USA) of the aqueous absorption media.

### 2.3.2. Organic analysis and ash measurement

Carbon, hydrogen, nitrogen, sulphur and oxygen content of the raw biomass and bio-coal was analysed using a Flash 2000 CHNS-O analyser (Thermo Scientific, USA). The instrument was calibrated and checked

using calibration standards and certified biomass reference materials (Elemental Microanalysis, UK). Ash content within the raw biomass and bio-coal was calculated using both ashing in a muffle furnace and thermo-gravimetric analysis (Mettler Toledo, Switzerland). Figures were given on a dry free basis, with hydrogen and oxygen values corrected to account for moisture. The 'as received' calorific value of the air dried bio-coal and freeze dried algae was calculated by bomb calorimetry (Parr, USA) and the higher heating value (HHV) subsequently calculated by Dulong's equation (see Eq. (1)).

$$\text{HHV} = (0.3383 * \% \text{Carbon}) + (1.422 * \% \text{Hydrogen}) - (\% \text{Oxygen} / 8) \quad (1)$$

### 2.3.3. Ash fusion testing

Ash fusion testing (AFT) was performed using a Carbolite digital ash fusion furnace. A digital camera is fixed to the front of the furnace to capture images of the illuminated ash while it is heated from 550 °C to 1570 °C at 7 °C minute<sup>-1</sup>. The tests were conducted in an oxidising atmosphere with an air flow of 50 ml minute<sup>-1</sup>. Cylindrical test pieces were formed using a dextrin binder (Sigma-Aldrich, USA) and were run in duplicate. Photographs were taken at 5 °C intervals but as the test was performed in accordance with the standard method for the determination of ash melting behaviour (DD CEN/TS 15370-1:2006) stages were given to the nearest 10 °C. The key stage temperatures are as follows: beginning of shrinkage (SST), sample deformation temperature (DT), hemisphere temperature (HT) and flow temperature (FT).

### 2.3.4. Predictive slagging and fouling indices

To predict the likelihood of fouling during combustion, various slagging and fouling indices have been derived based on the mean chemical composition of the fuels. The equations for alkali index (AI), bed agglomeration index (BAI), acid base ratio ( $R_a^b$ ), slagging (Babcock) index (SI), fouling index (FI), and slag viscosity index (SVI) are given as equations 1–6 in Table 1. For the AI an AI < 0.17 represents safe combustion, an AI > 0.17 < 0.34 predicts probable slagging and fouling and an AI > 0.34 predicts almost certain slagging and fouling [24]. For BAI, a value of BAI < 0.15 predicts that bed agglomeration is likely to occur [8]. For the  $R_a^b$  a value of < 0.5 indicates a low risk of slagging and an  $R_a^b$  > 1.0 predicts a high to severe risk of slagging during biomass combustion. SI values below SI < 0.6 predict a low slagging inclination, SI > 0.6 < 2.0 predicts a medium slagging inclination and SI > 2.0 predicts a high slagging inclination. For FI values below FI < 0.6 indicate a low fouling inclination FI > 0.6 < 40.0 medium fouling inclination and FI > 40.0 indicate high fouling inclination. An SVI > 72 indicates a low slagging indication where SVI > 63 < 72 suggests a medium indication and SIV < 65 indicates a high slagging inclination.

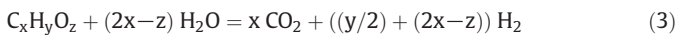
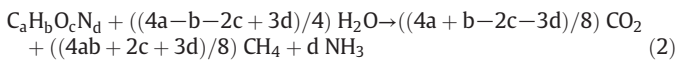
**Table 1**  
Predictive slagging and fouling indices.

Slagging/fouling index	Expression	Limit
Alkali index	$AI = \frac{Kg (K_2O + Na_2O)}{Cf}$	AI < 0.17 safe combustion AI > 0.17 < 0.34 probable slagging and fouling AI > 0.34 almost certain slagging and fouling
Bed agglomeration index	$BAI = \frac{\% (Fe_2O_3)}{\% (K_2O + Na_2O)}$	BAI < 0.15 bed agglomeration likely
Acid base ratio	$R_a^b = \frac{\% (Fe_2O_3 + CaO + MgO + K_2O + Na_2O)}{\% (SiO_2 + TiO_2 + Al_2O_3)}$	$R_a^b$ < 0.5 low slagging risk
Slagging index	$SI = \left( \frac{\% (Fe_2O_3 + CaO + MgO + K_2O + Na_2O)}{\% (SiO_2 + TiO_2 + Al_2O_3)} \right) * \% S(\text{dry})$	SI < 0.6 low slagging inclination SI > 0.6 < 2.0 medium slagging inclination SI > 2.0 high slagging inclination
Fouling index	$FI = \left( \frac{\% (Fe_2O_3 + CaO + MgO + K_2O + Na_2O)}{\% (SiO_2 + TiO_2 + Al_2O_3)} \right) * \% (K_2O + Na_2O)$	FI < 0.6 low fouling FI > 0.6 < 40.0 medium fouling FI > 40.0 indicate high fouling
Slag viscosity index	$SVI = \frac{\% (SiO_2 + 100)}{\% (SiO_2 + MgO + CaO + Fe_2O_3)}$	SVI > 72 low slagging indication SVI > 63 < 72 medium slagging indication SIV < 65 high slagging inclination

### 2.3.5. Process water analysis

The carbon content of the process water was analysed using a total organic carbon analyser (TOC) (Hach, Germany). Free ionic salts in the process waters were analysed by ion exchange chromatography (Dionex, USA). The organic compounds within the process waters were analysed by High Pressure Liquid Chromatography (HPLC) using three columns; (i) size exclusion column (Ultrasphere Gel with 0.1 M Na<sub>2</sub>NO<sub>3</sub> eluent) to show the size distribution of organic compounds present, (ii) organic acids' column (SupelcoGel C<sub>6-10</sub>-H with 1% H<sub>2</sub>PO<sub>4</sub> eluent) and (iii) sugars' column (SupelcoGel Pb with distilled water eluent). Quantification of known compounds was possible using a range of calibration standards (Sigma-Aldrich, USA).

The carbon, hydrogen, nitrogen and sulphur content of the process water was calculated by drying a known volume of process water at 60 °C over a period of 48 h to reduce loss of volatile organic compounds and the dried sample analysed using a Flash 2000 CHNS analyser (Thermo Scientific, USA). Inorganic content within the process water was calculated by heating to 550 °C in a muffle furnace in air, with oxygen calculated by difference. A process water yield was calculated based on the dried mass of the process water proportional to the mass of the starting biomass. Calculations of potential gas yields by methanogenesis have been calculated based on Boyle's equation (see Eq. (2)) and hydrogen yields via hydrogenesis using Eq. (3), with a, b, c, d and x, y, z being the molar fraction.



### 2.3.6. Experimental replication and statistical treatment

Hydrothermal carbonisation experiments that have been performed in duplicate were possible and the repeatability in yields is typically  $\pm 3$  wt.%. All analyses of product streams (bio-coal, process water, ash fusion testing, proximate and ultimate analyses) were performed in duplicate. Average values are reported together with standard error in tables and figures. In addition, analysis using TOC and ICP is based on multiple sample injections until a maximum standard deviation of  $\pm 2\%$  is achieved. For colorimetric analysis, absorbance readings were taken in triplicate and the mean value is reported.

## 3. Results and discussion

### 3.1. Influence of HTC on the bio-coal organic chemistry

The mass yields, calorific content and elemental composition of the starting seaweed and resulting bio-coals are given in Table 2. The results have shown a significant increase in energy density in the bio-coal, with the 'as received' calorific value (CV) of the fuel typically 22 MJ/kg for the 200 °C treatment and 25 MJ/kg for the 250 °C treatment. The CV of the initial feedstock typically ranges from 11.2 and 14.1 MJ/kg. It should be noted that the starting biomass has been dried, with a starting moisture content of between 80 and 90%, this energy penalty has not been considered in these figures, the bio-coals on the other hand have merely been air dried, with an air dried moisture content of between 2.1 and 3.5%. The energy densification of the bio-coals appears to be as a result of changes to the ratio of carbon and oxygen (O/C) in the fuel, with the carbon content appearing to increase, while the oxygen and ash content appears to decrease. The Van Krevelen diagram given in Fig. 1 shows how the O/C and hydrogen to carbon (H/C) ratios of the bio-coals compare with coals and lignin [20,38]. The results show that the bio-coals have a morphology with an O/C ratio between that of bituminous coals and lignite as reported in Hatcher et al. [18], although the O/C ratios are similar to reported pine and fir 255 °C bio coals reported in Hoekman et al. [20]. The H/C ratios are greater for the seaweed bio-coals than for coal, with all bio-coals typically between 0.9 and 1.3. This appears consistent with the H/C ratios presented in Smith et al. [39] where lignocellulosic biomass was processed under identical conditions, while Hoekman et al. [20] reported H/C ratios between 0.8 and 1.0 for their 255 °C bio-coals. High H/C ratios can however be associated with processing in alkaline conditions, as expected in seaweed due to the presence of alkaline metals [29]. The 250 °C seaweed bio-coals have a lower O/C ratio than the 200 °C seaweed bio-coals, as would be expected with lignocellulosic bio-coals. The H/C ratios for seaweed bio-coals are similar at each temperature, which differ from lignocellulosic biomass, where the lower temperature bio-coals had both higher O/C and H/C ratios [20]. The reductions in the H/C and the oxygen to carbon O/C ratios are also evidence that the seaweed bio-coals have undergone removal of hydroxyl groups through dehydration, removal of carboxyl and carbonyl groups through decarboxylation, and cleavage of many ester and ether bonds through hydrolysis as have been described in many publications which look into the HTC of lignocellulosic biomass [14].

Although the bio-coals have undergone energy densification similar to that of lignocellulosic biomass, the yields appear to be lower for macroalgae than lignocellulosic biomass. The yields for the

**Table 2**  
Proximate and ultimate analysis results for feedstock and bio-coals.

Feedstock	Yield (% mass)	% C (db)	% H (db)	% N (db)	% S (db)	% O (db)	HHV (Dulong) (MJ/kg)	CV (Bomb) (MJ/kg) (ar)	% Ash (db)	H/C (daf)	O/C (daf)
<i>Alaria</i>	–	38.2 $\pm$ 1.0	5.0 $\pm$ 0.3	2.3 $\pm$ 0.1	1.3 $\pm$ 0.1	30.9 $\pm$ 0.8	14.5	12.8	22.3 $\pm$ 0.0	1.57	0.61
HTC 200	30.0	58.0 $\pm$ 1.1	5.3 $\pm$ 0.2	3.4 $\pm$ 0.1	0.3 $\pm$ 0.0	23.8 $\pm$ 0.3	22.9	22.9	9.2 $\pm$ 0.3	1.09	0.31
HTC 250	23.7	59.1 $\pm$ 1.1	5.6 $\pm$ 0.1	3.3 $\pm$ 0.1	0.3 $\pm$ 0.1	17.3 $\pm$ 0.3	24.8	24.7	14.5 $\pm$ 0.2	1.13	0.22
<i>L. digitata</i>	–	33.3 $\pm$ 2.4	4.7 $\pm$ 0.2	1.7 $\pm$ 0.1	0.9 $\pm$ 0.3	31.1 $\pm$ 2.1	12.4	11.4	28.3 $\pm$ 0.0	1.70	0.70
HTC 200	21.8	50.2 $\pm$ 0.4	5.3 $\pm$ 0.1	2.4 $\pm$ 0.0	0.7 $\pm$ 0.1	20.1 $\pm$ 0.7	21.0	22.5	21.2 $\pm$ 0.3	1.27	0.30
HTC 250	18.4	55.9 $\pm$ 0.6	6.1 $\pm$ 0.0	2.9 $\pm$ 0.0	0.1 $\pm$ 0.0	26.6 $\pm$ 1.2	22.9	22.6	8.3 $\pm$ 0.1	1.31	0.36
<i>L. hyperborea</i> ' spring	–	32.3 $\pm$ 0.4	4.5 $\pm$ 0.1	2.7 $\pm$ 0.0	0.9 $\pm$ 0.6	29.3 $\pm$ 2.0	12.2	11.2	30.1 $\pm$ 0.0	1.69	0.68
HTC 200	28.6	54.2 $\pm$ 0.3	5.6 $\pm$ 0.0	3.5 $\pm$ 0.0	0.1 $\pm$ 0.0	24.7 $\pm$ 0.3	21.9	21.9	11.9 $\pm$ 0.1	1.24	0.34
HTC 250	24.7	54.0 $\pm$ 0.4	5.8 $\pm$ 0.0	3.1 $\pm$ 0.1	0.4 $\pm$ 0.1	19.8 $\pm$ 0.8	23.0	24.1	16.9 $\pm$ 0.2	1.29	0.28
<i>L. hyperborea</i> ' summer	–	38.2 $\pm$ 0.1	5.3 $\pm$ 0.0	1.9 $\pm$ 0.0	0.6 $\pm$ 0.0	33.3 $\pm$ 0.7	14.5	12.9	20.6 $\pm$ 0.0	1.67	0.65
HTC 200	31.2	62.3 $\pm$ 0.9	5.4 $\pm$ 0.2	3.1 $\pm$ 0.0	0.1 $\pm$ 0.0	24.8 $\pm$ 0.2	24.4	23.0	4.3 $\pm$ 0.1	1.05	0.30
HTC 250	24.3	67.1 $\pm$ 0.9	5.7 $\pm$ 0.1	3.2 $\pm$ 0.1	0.1 $\pm$ 0.0	18.2 $\pm$ 0.4	27.5	26.5	5.7 $\pm$ 0.1	1.01	0.20
<i>L. Hyperborea</i> ' autumn	–	42.0 $\pm$ 0.5	6.2 $\pm$ 0.1	2.0 $\pm$ 0.0	0.0 $\pm$ 0.0	39.5 $\pm$ 0.0	16.1	14.1	10.2 $\pm$ 0.0	1.78	0.70
HTC 200	33.0	64.6 $\pm$ 0.6	5.0 $\pm$ 0.0	2.6 $\pm$ 0.0	0.0 $\pm$ 0.0	24.1 $\pm$ 0.4	24.7	22.6	3.6 $\pm$ 0.1	0.93	0.28
HTC 250	31.7	66.9 $\pm$ 0.3	5.0 $\pm$ 0.1	2.8 $\pm$ 0.1	0.0 $\pm$ 0.0	20.1 $\pm$ 0.2	26.2	25.9	5.1 $\pm$ 0.1	0.90	0.23
<i>L. Hyperborea</i> ' winter	–	34.5 $\pm$ 0.2	4.8 $\pm$ 0.0	2.4 $\pm$ 0.0	0.0 $\pm$ 0.0	29.3 $\pm$ 0.9	13.2	12.3	29.1 $\pm$ 0.0	1.66	0.64
HTC 200	39.0	57.8 $\pm$ 0.8	4.9 $\pm$ 0.1	3.1 $\pm$ 0.0	0.1 $\pm$ 0.0	23.3 $\pm$ 0.8	22.3	21.2	10.8 $\pm$ 0.2	1.01	0.30
HTC 250	23.6	63.3 $\pm$ 0.9	5.5 $\pm$ 0.2	3.3 $\pm$ 0.1	0.1 $\pm$ 0.0	16.5 $\pm$ 0.2	26.3	25.4	11.3 $\pm$ 0.1	1.04	0.20

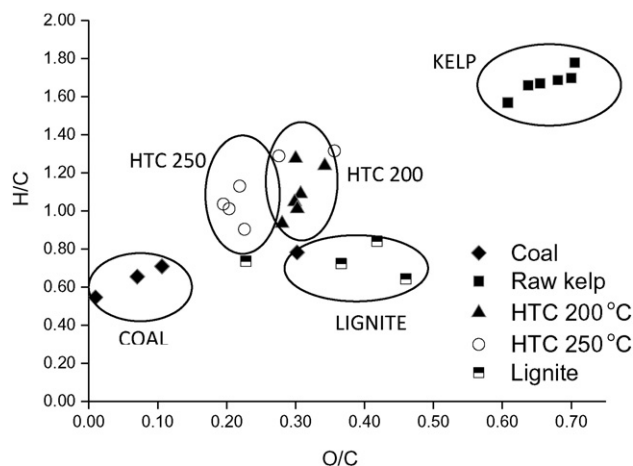


Fig. 1. Van Krevelen diagram showing bio-coals, biomass, lignite and coals (lignite and coals adapted from Hatcher et al. [18]).

lignocellulosic biomass, processed under similar conditions range between 58% and 70% at the lower process temperature (200 °C) and between 40% and 46% for the higher process temperature (250 °C) for oak, willow and *Miscanthus* [39]. The low yields will largely be a result of differences in biochemical composition. Brown kelps, as processed, comprise largely of carbohydrate in the form of parallel chains of polymeric alginic acid along with mannitol, laminarin, fucoidan and other polysaccharides [35], while lignocellulosic material is derived of cellulose, hemicellulose and lignin.

HTC is a complex series of reactions which are not fully understood for macroalgae. It is however likely that macroalgae undergoes a series of initial degradation reactions including hydrolysis, decarboxylation and dehydration followed by secondary repolymerisation reactions as described for lignocellulosic biomass [20,28]. Dehydration and decarboxylation reactions remove carboxyl and hydroxyl groups leaving unsaturated compounds which can polymerise easily, resulting in condensation and polymerisation of oligomers and monomers derived from the hydrolysis of carbohydrates which also simultaneously undergo aromatisation and condense onto the aromatic macromolecule [14]. It is however unclear whether there is a macromolecule structure which remains to which the reformed compounds can adhere. Jeon et al. [25] have looked into the hydrothermal degradation of sodium alginate, a water soluble alginate, at 200 °C and 250 °C using acid and base catalysts and did not report a char yield. The results showed that depolymerisation of alginic acid occurs from 150 °C; with hydrolysis converting the sodium alginate to monomers followed by subsequent reformation to organic acids, predominantly furfural, glycolic acid and formic acid. This result would imply that the soluble sodium and potassium alginate will decompose during HTC; however the behaviour of calcium and magnesium alginate will be somewhat different. Divalent cations, such as calcium and magnesium, when associated with alginate form water insoluble alginates and bind preferentially to the poly-guluronic acid units of alginate forming stable cross-linking chains and the addition of calcium chloride to hydrothermally carbonised alginate has been shown to promote the formation of carbon microspheres by exploiting this [11]. Consequently it is possible that calcium and magnesium play an important role in the formation of the bio-coals during HTC of macroalgae, with the divalent cations present in the process waters nucleating alginate hydrolysis fragments and forming nuclei from which the bio-coals can grow. This theory is supported by the metal analysis of the bio-coals (see Fig. 2), which showed the calcium and magnesium increase in concentration within the bio-coals while the potassium and sodium are extracted. The formation of carbon microspheres from alginate indicates that seaweeds form in a similar manner to that of non-crystalline cellulose derived chars. Subsequently

optimising char yield will depend mainly on the carbonisation time and concentration, which are determined by the water to solids ratio [6,40].

### 3.2. Influence of HTC on the bio-coal ash chemistry

While HTC appears to overcome the issues of moisture content and calorific value associated with seaweeds, the main issue which prevents its utilisation in combustion, pyrolysis or gasification is the high chlorine, high ash and high alkali metal content which results in very unfavourable ash chemistry in terms of slagging, fouling, bed agglomeration and corrosion [35].

Slagging is a phenomenon brought about through the melting of ash when ash deposits are exposed to radiant heat, such as flames in a furnace. As most furnaces are designed to remove ash as a powdery residue, having a high ash melting temperature is often desirable as it fuses into a hard glassy slag, known as a clinker, extraction is difficult and the furnace requires cleaning [27]. Bed agglomeration is similar to slagging but is an issue specific to fluidised bed furnaces and comes about through the formation of potassium silicates within the ash which melt and lead to adhesion of the bed material [16]. For slagging and bed agglomeration, the temperature at which the ash melts and fuses is strongly influenced by the alkali and alkaline metals which act as a flux for alumina-silicate ash [27]. Fouling is brought about when potassium and sodium, in combination with chlorine, partially evaporate when exposed to radiant heat and form alkali chlorides which condense on cooler surfaces such as heat exchangers. These deposits don't just reduce heat exchanger efficiency; they also play a major role in corrosion as these deposits react with sulphur in the flue gas to form alkali sulphates releasing chlorine in the process. This chlorine has a catalytic effect which results in the active oxidation and corrosion of the furnace material [27]. Consequently to reduce the propensity for an ash to slag or foul it is important to minimise the alkaline earth metals, particularly potassium and sodium within the ash along with chlorine and other halogens.

Fig. 2 shows the main ash forming elements within the bio-coal and feedstock and Table 3 shows the percentage of metals extracted. Extraction efficiency is calculated by multiplying the concentration (ppm) of metal within the bio-coal with the product yield to give mg metal remaining per kg of feed. This is then divided by the initial feedstock concentration to give percentage removal. Results show that sodium is extracted in excess of 99% for both treatments, with potassium extraction in the region of 97% at 200 °C and 99% at 250 °C. Chlorine is also removed in high quantities, typically around 99% with slightly higher extraction associated with the increased reaction severity. The extraction efficiency of calcium and magnesium is less than the alkaline metals, with the higher temperature treatments extracting less calcium and magnesium than the 200 °C hydrotreatment. This would suggest that these divalent cations are either being retained by the bio-coal through the increased surface functionality of the chars created at high temperature retaining these cations through cation exchange [28] or play a key role in the formation of microspheres of char [11] which act as nuclei around which the bio-coal can form.

While the extraction efficiency of the HTC process is interesting, the resulting concentration of metals and heteroatoms within the bio-coal is what is actually important and these results are given in Fig. 2. The results show significant reductions in the net concentrations of sodium, magnesium and chlorine which will bring significant benefits in terms of the slagging and fouling properties of the char. The results show a net increase in the concentrations of the two divalent cations within the bio-coal, with magnesium concentration reducing in the 200 °C bio-coal but increasing in the 250 °C bio-coal. The increase in magnesium concentration is far greater than the decrease in mass yield at the higher temperature which shows that magnesium is being re-uptaken at the higher temperatures, either due to increasing surface functionality or because at the higher temperatures it plays a role in

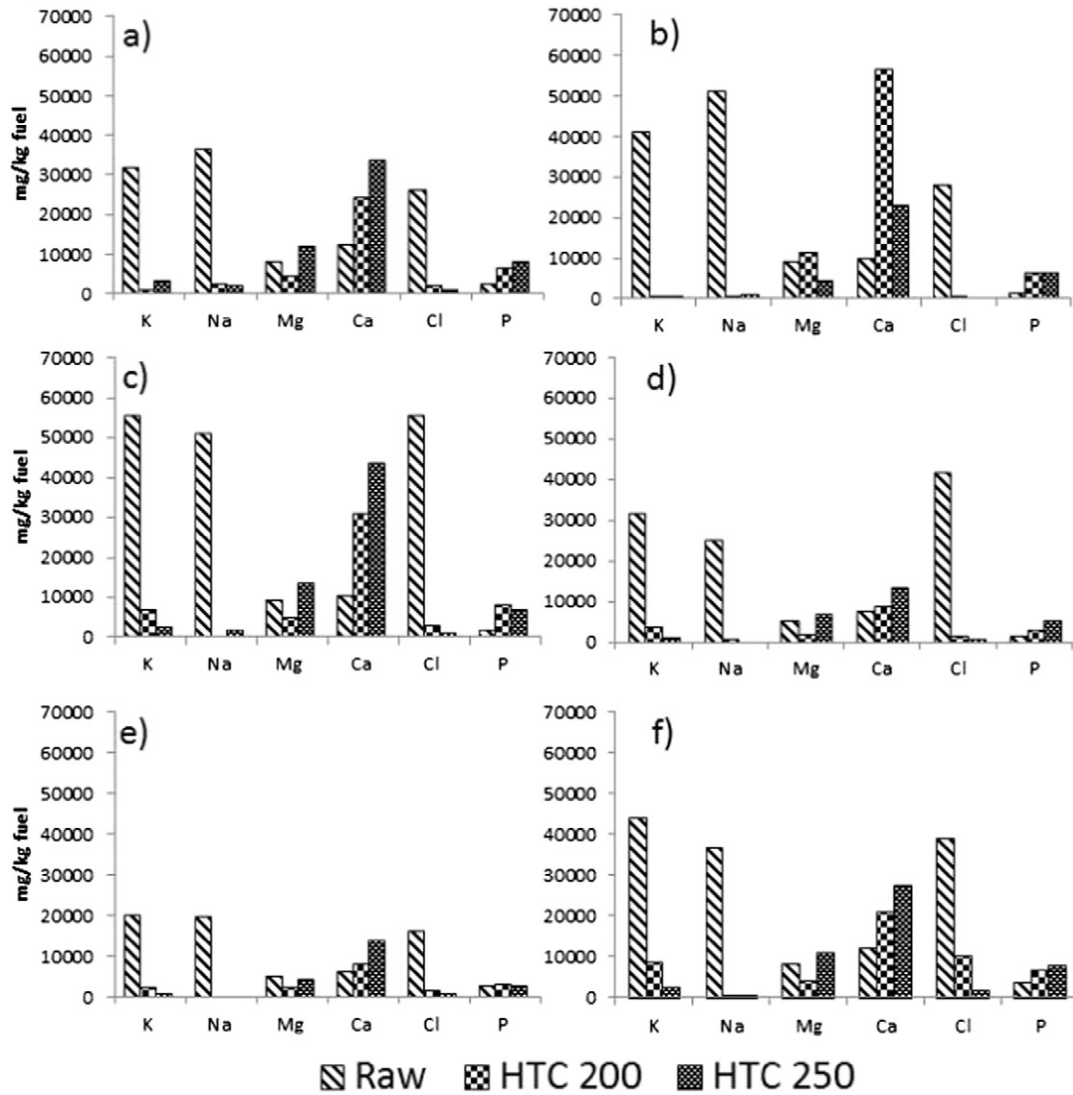


**Fig. 2.** Concentrations of the main ash forming elements within the raw kelps and corresponding bio-coals. a) *A. esculenta* (summer), b) *L. digitata* (summer), c) *L. hyperborea* spring harvest, d) *L. hyperborea* summer harvest, e) *L. hyperborea* autumn harvest and f) *L. hyperborea* winter harvest (concentrations and standard error of mean are given in supplementary materials Table 3).

the bio-coal formation. The calcium concentration increases in both treatments but to a greater extent in the 250 °C hydrothermal treatment. As calcium's uptake is different to that of magnesium, it appears likely

that calcium is playing a role in the bio-coal formation with its role increasingly important at higher temperatures. It has generally been observed that phosphorous is a controlling element in the ash

**Table 3**  
Percentage extraction of the main problematic ash forming elements within the raw kelps.

	K (%)	Na (%)	Mg (%)	Ca (%)	Cl (%)	P (%)
<i>A. esculenta</i>	–	–	–	–	–	–
HTC 200	99.2 ± 0.1	98.4 ± 0.0	87.4 ± 1.2	56.1 ± 2.2	98.2	44.6 ± 6.8
HTC 250	98.1 ± 0.3	99.0 ± 0.0	73.3 ± 0.4	51.2 ± 1.1	99.3	44.3 ± 2.2
<i>L. digitata</i>	–	–	–	–	–	–
HTC 200	99.8 ± 0.0	99.8 ± 0.0	82.6 ± 0.3	19.5 ± 1.8	99.8	36.0 ± 7.7
HTC 250	99.8 ± 0.0	99.8 ± 0.0	93.7 ± 0.1	69.6 ± 0.6	99.9	40.9 ± 10.8
<i>L. hyperborea</i> ' spring	–	–	–	–	–	–
HTC 200	97.7 ± 0.4	99.9 ± 0.0	89.4 ± 0.5	44.5 ± 2.9	99.0	16.5 ± 2.2
HTC 250	99.3 ± 0.0	99.5 ± 0.0	76.8 ± 0.2	35.1 ± 2.1	99.7	39.9 ± 2.8
<i>L. hyperborea</i> ' summer	–	–	–	–	–	–
HTC 200	97.4 ± 0.7	99.3 ± 0.0	92.7 ± 0.8	75.3 ± 1.4	99.2	61.0 ± 3.8
HTC 250	99.4 ± 0.1	99.6 ± 0.0	77.5 ± 0.3	68.0 ± 1.6	99.7	39.7 ± 1.2
<i>L. hyperborea</i> ' autumn	–	–	–	–	–	–
HTC 200	96.8 ± 1.5	99.8 ± 0.0	86.9 ± 2.0	61.9 ± 6.3	97.5	66.5 ± 6.3
HTC 250	99.3 ± 0.0	99.7 ± 0.0	78.2 ± 1.5	43.2 ± 5.1	98.7	73.1 ± 5.0
<i>L. hyperborea</i> ' winter	–	–	–	–	–	–
HTC 200	94.5 ± 0.0	99.6 ± 0.0	86.8 ± 0.6	52.0 ± 0.3	92.8	48.2 ± 0.3
HTC 250	98.8 ± 0.2	99.6 ± 0.0	72.3 ± 1.4	52.8 ± 0.5	99.1	53.3 ± 1.4

**Table 4**  
Fouling indices and ash fusibility flow temperature.

Feedstock	Fouling and slagging indices ash fusion								
	AI	BAI	R b/a	SI	FI	SVI	Deformation (°C)	Flow (°C)	Notes
<i>A. esculenta</i>	6.86	0.81	68.25	84.1	2793.5	2	620	>1570	Tile deformed
HTC 200	0.12	0.28	6.17	0.0	19.1	10	1450	1490	
HTC 250	0.27	0.66	12.76	1.0	61.0	4	1470	1550	
<i>L. digitata</i>	10.48	0.64	300.66	232.0	14,139.8	0	550	1220	
HTC 200	0.07	0.61	35.20	0.3	26.8	1	1450	1490	
HTC 250	0.08	0.45	16.66	0.0	38.3	2	1260	1540	
<i>L. hyperborea</i> ' spring	12.13	0.27	197.38	170.3	9297.6	1	570	610	
HTC 200	0.38	0.46	17.27	0.2	135.7	5	1540	>1570	
HTC 250	0.22	0.43	33.59	1.6	109.8	3	>1570	>1570	
<i>L. hyperborea</i> ' summer	5.56	0.38	165.97	107.4	5763.1	1	550	680	
HTC 200	0.23	0.56	9.55	1.6	134.2	11	>1570	>1570	
HTC 250	0.07	0.61	15.83	0.9	56.6	5	>1570	>1570	
<i>L. hyperborea</i> ' autumn	3.61	0.56	467.72	8.3	24,757.7	0	<790	1520	Tile deformed
HTC 200	0.13	1.05	29.62	0.0	265.7	4	1480	1530	
HTC 250	0.04	0.94	49.87	0.4	103.4	2	>1570	>1570	
<i>L. hyperborea</i> ' winter	8.36	0.51	354.96	12.4	12,295.2	0	<800	1090	
HTC 200	0.50	0.45	27.32	1.0	297.7	3	1470	1510	
HTC 250	0.15	0.48	36.44	4.5	132.3	2	>1570	>1570	

transformation reactions during biomass combustion due to the high thermal stability of phosphate compounds [16] and consequently this may improve the ash behaviour. The presence of phosphates within the bio-coal (results given as elemental phosphorus) would indicate that a portion of the metals within the bio-coal are metal phosphates which will have higher thermal stability when compared to metal oxides and thus improved ash behaviour.

The slagging and fouling indices for the seaweeds and corresponding bio-coals are given in Table 4. It is worth noting that the ash chemistry in the seaweeds is very different to that of a bituminous coal, which is predominantly comprised of silicon dioxide, iron oxide and aluminium oxide, while the ash of unprocessed raw kelp is largely alkali or alkaline earth metal salts. The large composition of alkali and alkaline earth metals results in an alkaline ash, which is why the acid base ratios are very high as both the raw feedstock and the bio-coals have very low aluminium, silicon and titanium content resulting in base heavy ash. Likewise the low silicon content results in low values for the slag viscosity index which implies that there may be issues with slagging based on the viscosity of the ash. The results for the slagging indices show significant improvement in slagging propensity, with the slagging indices showing that the higher temperature bio-coals are safe for combustion, whereas the raw seaweeds are not. This is consistent with the results of the ash fusion testing which have shown significant improvements in all the transition temperatures (see Fig. 3), with all the *L. hyperborea* 250 °C bio-coals not even deforming before exceeding the furnace limit of 1570 °C, deformation being the point when the ashes generally start becoming sticky and potentially problematic. The raw *L. hyperborea* ashes have been shown to deform at 560 °C or below and go to flow (melt) at temperatures as low as 610 °C, which shows how the fuel has been transformed from a high slagging fuel to a fuel with a low slagging potential [27]. The 250 °C bio-coals for *A. esculenta* and *L. digitata* started to deform at 1470 °C and 1260 °C and both went to flow but at temperatures 1550 °C and 1540 °C respectively but these would be regarded as high deformation and melting temperatures. The 200 °C bio-coals melted at lower temperatures than the 250 °C bio-coals, with *A. esculenta* and *L. digitata* and *L. hyperborea*; autumn and winter samples melting at 1490, 1490, 1530, and 1510 °C respectively, but had similar deformation temperatures to the 250 °C bio-coals, deforming at 1450, 1450, 1480 and 1470 °C respectively. *L. hyperborea* spring 200 °C bio-coal had gone to deformation at the furnace limit (1570 °C) but not gone to hemisphere or flow. *L. hyperborea* summer 200 °C bio-coal had merely shrunk by the furnace limit (1570 °C). High flow temperatures were observed for the raw *A. esculenta* and *L. hyperborea* autumn samples, which would indicate a low slagging propensity, but the low deformation temperatures of

620 °C and <550 °C for the raw samples would indicate that they would be highly problematic. For the raw *A. esculenta* and *L. hyperborea* autumn samples the ceramic tiles on which the test pieces were placed were severely corroded and warped. This was not observed for any of the bio-coal test pieces.

While the ash fusion furnace indicates the propensity of an ash to slag, it does not indicate the propensity for a fuel to foul. The fouling index is given in Table 4 and suggests a high fouling propensity for all bio-coals. Some caution is needed when interpreting this as indices have been developed for coal and make assumptions on the coal mineralogy which are very different to the mineralogy of the bio-coals [27]. For example it is shown in Fig. 2 that a large portion of the chlorine has been extracted during the HTC process, with chlorine playing an important role in the fouling and corrosion mechanism [33]. The fouling indices make assumptions on the mineralogy of the fuel in particular the chlorine content of the fuel; hence it is not used in the derivation of the fouling risk [27]. There are also assumptions that the salts are simply metal oxides whereas, as shown with the high bio-coal phosphorous concentrations it is more than likely that some of the metals are metal phosphates which have far greater thermal stability [16]. Thus the bio-coals may, in practice, be low fouling but the presence of alkali and alkaline earth metals will always result in it being highlighted as having a high fouling risk when using coal derived fouling indices. This said, significant shrinkage of all the test pieces was observed which could indicate volatilisation of compounds within the ash, possibly potassium and sodium which could lead to fouling. Consequently understanding of how the bio-coal ash chemistry changes as it is heated is a significant future step in determining the suitability of seaweed bio-coals in combustion. Ash fusion testing of the raw seaweed ashes resulted in significant fouling of the furnace optics which confirms the findings of Ross et al. [35] that fouling will be a significant problem when combusting seaweeds without pre-treatment.

### 3.3. Process water chemistry

The anions and cations within the process waters were analysed by ion chromatography (IC) and the results are shown in Table 5. The process water contains high concentrations of sodium and potassium along with high concentrations of the associated halogens; chlorine, fluorine and bromine. This correlates with the reductions seen in the bio-coal, which indicate that the fate of the alkali metals and their associated anions is the process water. The divalent cations magnesium and calcium are also present within the process water although they are present in significantly lower concentrations, with approximately 5 g of calcium per kg of feedstock, whereas potassium varies between 30 and 83 g/kg

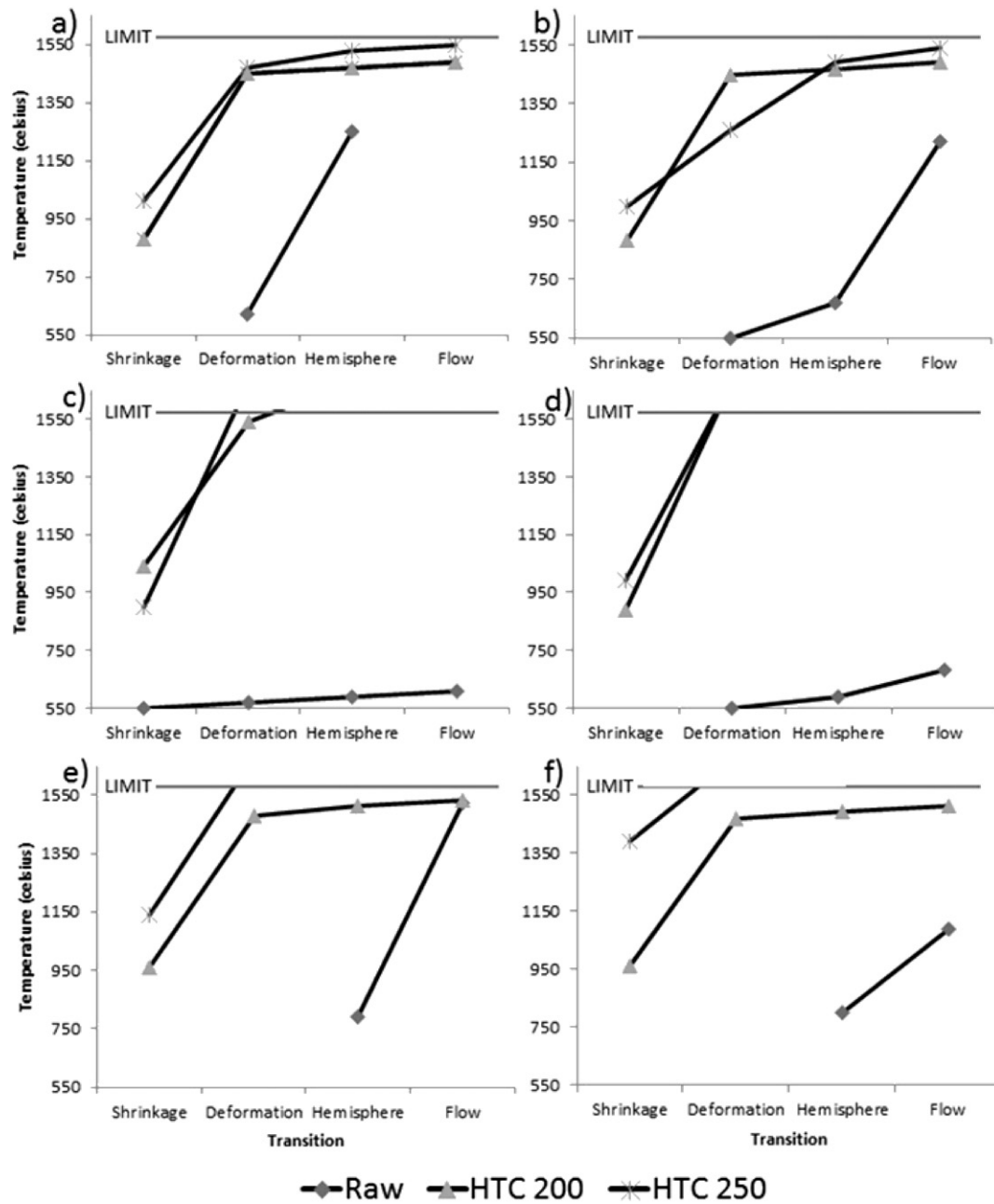


Fig. 3. Ash fusion transition temperatures for the raw kelps and corresponding bio-coals. a) *A. esculenta* (summer), b) *L. digitata* (summer), c) *L. hyperborea* spring harvest, d) *L. hyperborea* summer harvest, e) *L. hyperborea* autumn harvest and f) *L. hyperborea* winter harvest.

Table 5

Mass (g) of anions, cations and organic carbon in the process water after HTC of 1 kg feedstock using 10:1 water to solids ratio.

Sample	Anions process water (g/kg feed)						Cations process water (g/kg feed)					Organic carbon
	F <sup>-</sup>	Cl <sup>-</sup>	NO <sub>2</sub> <sup>-</sup>	Br <sup>-</sup>	NO <sub>3</sub> <sup>-</sup>	PO <sub>4</sub> <sup>3-</sup>	Na <sup>+</sup>	NH <sub>4</sub> <sup>+</sup>	K <sup>+</sup>	Mg <sup>2+</sup>	Ca <sup>2+</sup>	
<i>A. esculenta</i> 200	6.9	53.0	0.2	0.2	2.3	30.5	32.7	2.2	29.7	5.6	4.9	148.1
<i>A. esculenta</i> 250	2.6	53.3	0.2	0.8	1.6	24.1	29.5	4.2	34.8	4.0	3.7	155.8
<i>L. digitata</i> 200	8.6	65.7	0.5	1.9	2.3	35.7	37.1	0.0	40.8	6.5	5.9	177.1
<i>L. digitata</i> 250	4.7	58.5	0.5	1.9	2.2	11.6	39.0	0.0	41.7	6.8	5.9	160.6
<i>L. hyperborea</i> ' spring 200	5.9	81.0	0.5	10.7	0.9	44.6	36.9	2.0	43.0	5.8	2.5	100.1
<i>L. hyperborea</i> ' spring 250	4.8	69.8	0.4	10.4	2.4	23.7	40.6	3.9	68.9	5.8	3.4	124.9
<i>L. hyperborea</i> ' summer 200	2.7	24.7	0.5	1.0	1.3	29.0	19.3	1.6	33.8	3.3	3.7	154.1
<i>L. hyperborea</i> ' summer 250	5.3	33.3	0.5	1.2	2.3	41.1	20.5	1.0	37.8	4.2	4.4	182.9
<i>L. hyperborea</i> ' autumn 200	5.3	18.4	0.4	1.0	2.3	26.2	18.0	0.0	20.1	4.1	3.6	148.0
<i>L. hyperborea</i> ' autumn 250	1.8	2.3	0.0	0.9	0.9	15.3	14.4	0.9	22.4	3.0	2.2	138.7
<i>L. hyperborea</i> ' winter 200	7.3	64.6	0.5	4.7	2.5	64.1	26.4	3.8	75.3	5.5	3.5	87.2
<i>L. hyperborea</i> ' winter 250	4.4	76.0	0.5	4.9	1.0	75.7	25.9	6.0	83.3	4.2	3.1	105.0



feedstock depending on the species and the season. In addition to the high cations present, there are also high concentrations of phosphate present within the process waters with concentrations varying from 12 g/kg feedstock to 76 g/kg feedstock. The presence of potassium and phosphate in high concentrations and to a lesser extent calcium and magnesium raises the prospect of recovering these salts for use in fertilizer. Current mean market price (July 2015) for processed di-ammonium phosphate (DAP) is \$473 tonne, and potassium chloride fertilizer is \$307, unprocessed the wholesale value of crude potash \$300 tonne and phosphate rich rock \$115 tonne in July 2015. While this paper does not attempt to suggest potential extraction routes; for HTC of macroalgae to develop to a commercial scale it is essential to identify applications which offer technical or economic advantages over conventional biomass processes and the recovery of essential plant nutrients would be one such route.

In addition to the salts present within the process water there is also nitrogen in the form of nitrite, nitrate and ammonia. This will be largely derived from the organically bound nitrogen within the macroalgae. Table 2 shows the nitrogen content of the bio-coal and indicates that a significant portion of the nitrogen is transferred to the process water resulting in only a slight increase in nitrogen in the bio-coal. The relatively low concentrations of nitrogen detected by IC is indicative that the remaining nitrogen is in the form of organic compounds such as nitrogen heterocycles, pyrroles and indoles in the process waters due to the degradation of proteins [9] along with Maillard reaction products due to interactions between the proteins and carbohydrates [19]. It is also likely that a number of organic compounds will also be associated with metals and heteroatoms which will not have been detected by IC. Consequently the metals and heteroatoms detected by IC should be taken as free ionic salts in the process waters and not the total extracted metals and heteroatoms.

Table 5 also shows the organic carbon within the process water, which is believed to be comprised of organic acids and possibly sugars but will also include the nitrogen containing organic compounds such as Maillard reaction products, nitrogen heterocycles, pyrroles and indoles. The yield in Table 5 has been standardised per kg of feedstock but it is likely that this figure will be increased by increasing the water to biomass ratio and decreased by reducing it as it appears that organic acids produced during HTC are equilibrium products [31]. HPLC was used to determine the likely composition of the process waters using a combination of HPLC and GPC. The results (shown in the Supplementary information) indicate that a large proportion of the organic compounds within the process waters have a molecular weight of around 340 Mw which would imply the presence of C6 compounds such as sugars. This accounts for typically around 80% of the organic compounds present. This however contradicts the findings of Anastasakis and Ross [4] who did not detect sugars following pyrolysis–gas chromatography at 250 °C although this is probably due to their low volatility. The low weight peak corresponds to the presence of organic acids accounting for around 20% of the organic material present as identified by HPLC. Analysis of the organic acids by HPLC confirms the presence of methyl-malonic acid, lactic acid and formic acid at high concentrations. Citric acid, acetic acid and levulinic acid were also detected at slightly lower concentrations.

The process waters from the HTC of macroalgae have been shown to be high in organic carbon, which on the one hand is to the detriment to the bio-coal yield but on the other hand could be an opportunity to recover high value chemicals or enhanced energy recovery. It is likely that higher bio-coal yields can be achieved by increasing the retention times, and reducing the water to biomass ratio as this has been demonstrated to increase the bio-coal product yields for non-crystalline cellulose [6, 40] and the results in Chen et al. [11] certainly indicate that alginate under HTC behaves like non-crystalline cellulose. This will however have a detrimental effect on the organic products within the process waters and possibly the extraction of heteroatoms. Many of the organic acids known to be present within the process water after hydrothermal

processing of macroalgae have a reasonable market value, possibly greater than the value of the additional bio-coal gained through modification of loadings and retention times. Consequently the feasibility of recovery of these organic acids needs further investigation.

Further exploitation of these organics within the process waters is required. In the simplest form this could be recycling of the organics back into the HTC process, exploiting the possible catalytic effects of the organic acids and salts [30,31], although extraction of salts would be required to avoid saturation. The second solution would be fermentation of the organic acids and sugars under anaerobic conditions. Wirth and Mumme [41] have demonstrated the AD of process waters from the HTC of corn silage, yielding methane. Inhibition could however be an issue with the mildly alkaline conditions, the presence of alkali cations and the presence of ammonia potentially inhibiting methanogenic bacteria [32] so the AD route may favour alternative routes such as hydrogen or ethanol production, or enhanced organic acid production via the carboxylate platform [3]. In order to assess the potential for enhanced energy recovery via AD, process waters were oven dried and underwent ultimate analysis. The theoretical hydrogen and methane yields calculated using Eqs. (2) and (3) are shown in Table 6. While these yields are theoretical maximums, it is likely that high conversions will be attained due to the organic material being simple organic acids and sugars [41]. Based on the results it appears that hydrogen production via AD would yield the higher energy yields and this route would be less likely to suffer nitrogen inhibition. This route is also potentially more favourable in terms of project economics as hydrogen yields are achieved through high throughput and short retention times which lead to smaller digesters and lower CAPEX [3]. Fig. 4 (1a, 1b, 2a, 2b) shows the potential net energy yields from HTC followed by AD using the hydrogen (1a and 1b) and methane route (2a and 2b), using a theoretical AD yield of 75% calculated by Boyle's equation, a modified version of the Buswell equation. It should be noted that the results given in Table 6 are for oven dried samples and a proportion of the organic material is potentially volatilised. The low sulphur content of the process water is indicative that volatile sulphated compounds have been volatilised in the drying process.

#### 3.4. Influence of seasonal variation in bio-chemical composition on product yield

The energy yields from HTC and AD of *L. hyperborea* harvested throughout the year are given in Fig. 4. The results show that there is significant variation between the three species and the time of year of harvest. *L. hyperborea* appears to give the highest yields of bio-coal, with *A. esculenta* giving the second highest yields. Interestingly the higher temperatures appear to give lower energy yields, which imply that despite increased energy densification of the products, this is offset by the significant decrease in yield. The reduced bio-coal energy yield due to the higher temperature treatment is however offset by the increased potential energy yield from either hydrogen or methane production via AD along with the improvements in slagging propensity of the solid fuel. The char yields appear highest in the autumn which correlates with the fuel having the highest carbon content [37] and the yields are lowest for material harvested in the spring, when ash is highest [2,37]. This high ash content in the early spring also makes the fuel, even once hydrotreated at 250 °C unsuitable for direct combustion due to fouling and slagging risk, although it still could be blended. The carbohydrate content of the algae, which peaks in the summer samples (July) [2,37] appears less important than maximum carbon in terms of maximum bio-coal yield, although the higher carbohydrate content in the feedstock appears to increase the hydrogen and methane yields obtained by AD, which offsets the reduced energy yields in the bio-coal.

In summary the results generally show that the highest energy yields are obtained in the summer and autumn harvested algae, however contrary to direct seaweed AD which is reliant on carbohydrate content [2], it is not necessary to harvest in July to obtain maximum yield

**Table 6**  
Ultimate analysis of oven dried process waters and their theoretical methane and hydrogen yields.

Feedstock	Starting solids in water (wt.%)	Ultimate analysis					g/kg feedstock		MJ/kg feedstock		
		% C	% H	% N	% S	% O (dif)	Ash %	H <sub>2</sub> (g)	CH <sub>4</sub> (g)	H <sub>2</sub>	CH <sub>4</sub>
		(db)	(db)	(db)	(db)	(db)	(db)	(120 MJ/kg)	(55 MJ/kg)		
<i>A. esculenta</i> 200	48.2	28.1 ± 2.0	5.1 ± 0.1	2.1 ± 0.1	0.6 ± 0.3	32.6	31.5	50.1	84.5	6.0	4.6
<i>A. esculenta</i> 250	49.2	30.5 ± 0.4	5.9 ± 0.1	1.8 ± 0.0	0.0 ± 0.0	32.0	29.8	59.1	85.4	7.1	4.7
<i>L. digitata</i> 200	57.7	26.9 ± 1.1	5.2 ± 0.1	1.3 ± 0.1	0.0 ± 0.0	34.1	32.5	57.0	96.0	6.8	5.3
<i>L. digitata</i> 250	57.1	31.4 ± 0.9	6.5 ± 0.2	1.4 ± 0.0	0.0 ± 0.0	33.3	27.5	73.0	96.3	8.8	5.3
<i>L. hyperborea</i> ' spring 200	50.1	15.3 ± 2.3	2.9 ± 0.6	2.3 ± 0.4	0.1 ± 0.1	37.5	41.8	16.6	74.1	2.0	4.1
<i>L. hyperborea</i> ' spring 250	47.1	18.8 ± 3.1	3.3 ± 0.6	1.8 ± 0.3	0.0 ± 0.0	32.9	43.2	25.6	70.3	3.1	3.9
<i>L. hyperborea</i> ' summer 200	46.3	32.0 ± 0.4	6.0 ± 0.1	1.5 ± 0.0	0.0 ± 0.0	38.2	22.3	55.2	90.0	6.6	4.9
<i>L. hyperborea</i> ' summer 250	55.3	32.0 ± 0.9	6.1 ± 0.4	1.5 ± 0.1	0.0 ± 0.0	34.8	25.6	68.5	102.5	8.2	5.6
<i>L. hyperborea</i> ' autumn 200	38.6	34.1 ± 0.3	6.3 ± 0.0	1.5 ± 0.0	0.0 ± 0.0	36.0	22.1	50.8	76.3	6.1	4.2
<i>L. hyperborea</i> ' autumn 250	37.1	31.7 ± 0.5	6.0 ± 0.1	1.6 ± 0.0	0.0 ± 0.0	46.4	14.4	39.8	79.7	4.8	4.4
<i>L. hyperborea</i> ' winter 200	44.5	21.3 ± 0.9	3.9 ± 0.2	2.8 ± 0.1	0.0 ± 0.0	23.5	48.5	35.9	60.1	4.3	3.3
<i>L. hyperborea</i> ' winter 250	46.2	17.0 ± 0.8	3.1 ± 0.2	2.2 ± 0.1	0.0 ± 0.0	21.5	56.2	28.2	52.7	3.4	2.9

when processing by HTC. HTC will allow harvesting throughout the summer and autumn which has the benefit of significantly extending the harvesting window and will enable harvesting to be coordinated with maximum biomass yield as opposed to optimum composition. The results do imply that harvesting in the spring is best avoided due to low yields and less favourable inorganic chemistry but if harvesting in the autumn overruns, harvesting in the early winter should not be too detrimental to the fuel inorganic chemistry but will have a penalty on yields.

#### 4. Conclusions

This study has shown that processing macroalgae via HTC can produce a coal like product with improved combustion properties. Moreover, hydrothermal carbonisation can overcome the highly unfavourable inorganic and heteroatom chemistry of macroalgae, which will otherwise largely prevent its utilisation in combustion, pyrolysis or gasification due to slagging, fouling and corrosion.

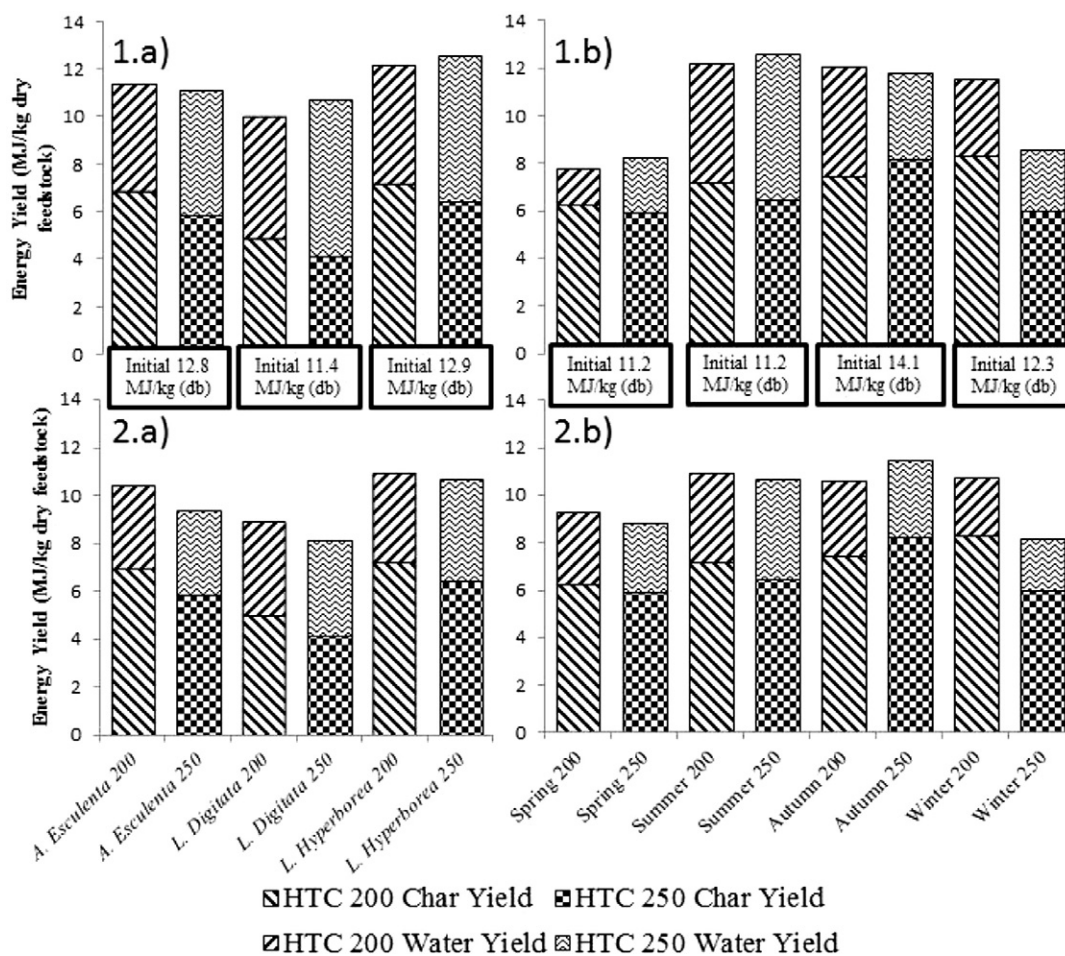


**Fig. 4.** Bio-coal, hydrogen (1) and methane (2) yields (75% of theoretical yield) from HTC followed by anaerobic digestion: 1a) variation between summer harvested species with hydrogenesis, 1b) variation between seasonal harvested *L. hyperborea* with hydrogenesis, 2a) variation between summer harvested species with methanogenesis, 2b) variation between seasonal harvested *L. hyperborea* with methanogenesis.

The results indicate that HTC can produce a coal like product with an enhanced energy density. The resulting bio-coal has a typical CV of 22 MJ/kg (ar) for the 200 °C treatment and 25 MJ/kg (ar) for the 250 °C treatment. HTC results in almost completely removes alkali metals and chlorine, the main elements responsible for slagging and fouling. Ash fusion testing has demonstrated that the slagging propensity of the resulting bio-coal is significantly reduced.

The process waters contain high concentrations of key plant nutrients; potassium and phosphorus, along with lower concentrations of calcium and magnesium and potentially exist for recovery and reuse of these minerals as a fertilizer. Anaerobic treatment of the process waters has the potential for recovery of energy as either methane or hydrogen. The combination of HTC and AD could retain 80% of the energy within the initial feedstock.

Consequently this study has shown that HTC is a promising pre-treatment for macroalgae producing a bio-coal with favourable combustion properties from a highly unfavourable feedstock. Further processing of the process water can generate bio-methane or, hydrogen and facilitate recovery of inorganics which will greatly improve the process economics.

### Acknowledgements

The authors would like to thank the EPSRC Doctoral Training Centre in Low Carbon Technologies (EP/G036608/1) for financial support of Aidan Smith and the European Commission for financial support of the 'Biorefine' project (320J Recycling inorganic chemicals from agro- & bio-industry wastestreams) for supporting Dr. Andrew Ross via the ERDF Interreg IVb NWE region programme. The authors would also like to thank Mr. Simon Lloyd and Dr. Adrian Cunliffe for their technical assistance.

### Appendix A. Supplementary data

Supplementary data to this article can be found online at <http://dx.doi.org/10.1016/j.algal.2016.02.026>.

### References

- [1] J. Adams, J. Gallagher, I. Donnison, Fermentation study on *Saccharina latissima* for bioethanol production considering variable pre-treatments, *J. Appl. Phycol.* 21 (2009) 569–574.
- [2] J.M.M. Adams, A.B. Ross, K. Anastasakis, E.M. Hodgson, J.A. Gallagher, J.M. Jones, I.S. Donnison, Seasonal variation in the chemical composition of the bioenergy feedstock *Laminaria digitata* for thermochemical conversion, *Bioresour. Technol.* 102 (2011) 226–234.
- [3] M.T. Agler, B.A. Wrenn, S.H. Zinder, L.T. Angenent, Waste to bioproduct conversion with undefined mixed cultures: the carboxylate platform, *Trends Biotechnol.* 29 (2011) 70–78.
- [4] K. Anastasakis, A.B. Ross, Hydrothermal liquefaction of the brown macro-alga *Laminaria saccharina*: effect of reaction conditions on product distribution and composition, *Bioresour. Technol.* 102 (2011) 4876–4883.
- [5] K. Anastasakis, A.B. Ross, Hydrothermal liquefaction of four brown macro-algae commonly found on the UK coasts: an energetic analysis of the process and comparison with bio-chemical conversion methods, *Fuel* 139 (2015) 546–553.
- [6] N. Baccile, G. Laurent, F. Babonneau, F. Fayon, M.-M. Titirici, M. Antonietti, Structural characterization of hydrothermal carbon spheres by advanced solid-state MAS 13C NMR investigations, *J. Phys. Chem. C* 113 (2009) 9644–9654.
- [7] Y.J. Bae, C. Ryu, J.-K. Jeon, J. Park, D.J. Suh, Y.-W. Suh, D. Chang, Y.-K. Park, The characteristics of bio-oil produced from the pyrolysis of three marine macroalgae, *Bioresour. Technol.* 102 (2011) 3512–3520.
- [8] D. Bapat, S. Kulkarni, V. Bhandarkar, Design and Operating Experience on Fluidized Bed Boiler Burning Biomass Fuels With High Alkali Ash, American Society of Mechanical Engineers, New York, NY (United States), 1997.
- [9] P. Biller, A.B. Ross, Potential yields and properties of oil from the hydrothermal liquefaction of microalgae with different biochemical content, *Bioresour. Technol.* 102 (2011) 215–225.
- [10] W. Black, The seasonal variation in weight and chemical composition of the common British Laminariaceae, *J. Mar. Biol. Assoc. U. K.* 29 (1950) 45–72.
- [11] J. Chen, Z. Chen, C. Wang, X. Li, Calcium-assisted hydrothermal carbonization of an alginate for the production of carbon microspheres with unique surface nanopores, *Mater. Lett.* 67 (2012) 365–368.
- [12] R. Cherad, J.A. Onwudili, P.T. Williams, A.B. Ross, A parametric study on supercritical water gasification of *Laminaria hyperborea*: a carbohydrate-rich macroalga, *Bioresour. Technol.* 169 (2014) 573–580.
- [13] E. Danso-Boateng, G. Shama, A. Wheatley, S. Martin, R. Holdich, Hydrothermal carbonisation of sewage sludge: effect of process conditions on product characteristics and methane production, *Bioresour. Technol.* 177 (2015) 318–327.
- [14] A. Funke, F. Ziegler, Hydrothermal carbonization of biomass: a summary and discussion of chemical mechanisms for process engineering, *Biofuels Bioprod. Biorefin.* 4 (2010) 160–177.
- [15] K. Gao, K. McKinley, Use of macroalgae for marine biomass production and CO<sub>2</sub> remediation: a review, *J. Appl. Phycol.* 6 (1994) 45–60.
- [16] A. Grimm, N. Skoglund, D. Boström, M. Ohman, Bed agglomeration characteristics in fluidized quartz bed combustion of phosphorus-rich biomass fuels, *Energy Fuel* 25 (2011) 937–947.
- [17] A. Gurung, S.W. Van Ginkel, W.-C. Kang, N.A. Qambrani, S.-E. Oh, Evaluation of marine biomass as a source of methane in batch tests: a lab-scale study, *Energy* 43 (2012) 396–401.
- [18] P.G. Hatcher, I.A. Breger, N. Szeverenyi, G.E. Maciel, Nuclear magnetic resonance studies of ancient buried wood—II. Observations on the origin of coal from lignite to bituminous coal, *Org. Geochem.* 4 (1982) 9–18.
- [19] S.M. Heilmann, L.R. Jader, M.J. Sadowsky, F.J. Schendel, M.G. von Keitz, K.J. Valentas, Hydrothermal carbonization of distiller's grains, *Biomass Bioenergy* 35 (2011) 2526–2533.
- [20] S.K. Hoekman, A. Broch, C. Robbins, Hydrothermal carbonization (HTC) of lignocellulosic biomass, *Energy Fuels* 25 (2011) 1802–1810.
- [21] S.J. Horn, *Bioenergy From Brown Seaweeds*, 2000.
- [22] S.J. Horn, I.M. Aasen, K. Østgaard, Ethanol production from seaweed extract, *J. Ind. Microbiol. Biotechnol.* 25 (2000) 249–254.
- [23] A.D. Hughes, M.S. Kelly, K.D. Black, M.S. Stanley, Biogas from macroalgae: is it time to revisit the idea? *Biotechnol. Biofuels* 5 (2012).
- [24] B. Jenkins, L. Baxter, T. Miles, Combustion properties of biomass, *Fuel Process. Technol.* 54 (1998) 17–46.
- [25] W. Jeon, C. Ban, G. Park, T.K. Yu, J.Y. Suh, H.C. Woo, D.H. Kim, Catalytic hydrothermal conversion of macroalgae-derived alginate: effect of pH on production of furfural and valuable organic acids under subcritical water conditions, *J. Mol. Catal. A Chem.* 399 (2015) 106–113.
- [26] K.A. Jung, S.-R. Lim, Y. Kim, J.M. Park, Potentials of macroalgae as feedstocks for biorefinery, *Bioresour. Technol.* 135 (2013) 182–190.
- [27] J. Koppejan, S. Van Loo, *The Handbook of Biomass Combustion and Co-firing*, Routledge, 2012.
- [28] J.A. Libra, K.S. Ro, C. Kammann, A. Funke, N.D. Berge, Y. Neubauer, M.M. Titirici, C. Fühner, O. Bens, J. Kern, K.H. Emmerich, Hydrothermal carbonization of biomass residuals: a comparative review of the chemistry, processes and applications of wet and dry pyrolysis, *Biofuels* 2 (2011) 71–106.
- [29] D. López Barreiro, M. Beck, U. Hornung, F. Ronsse, A. Kruse, W. Prins, Suitability of hydrothermal liquefaction as a conversion route to produce biofuels from macroalgae, *Algal Res.* 11 (2015) 234–241.
- [30] J.G. Lynam, C.J. Coronella, W. Yan, M.T. Reza, V.R. Vasquez, Acetic acid and lithium chloride effects on hydrothermal carbonization of lignocellulosic biomass, *Bioresour. Technol.* 102 (2011) 6192–6199.
- [31] J.G. Lynam, M. Toufiq Reza, V.R. Vasquez, C.J. Coronella, Effect of salt addition on hydrothermal carbonization of lignocellulosic biomass, *Fuel* 99 (2012) 271–273.
- [32] R. Rajagopal, D.I. Massé, G. Singh, A critical review on inhibition of anaerobic digestion process by excess ammonia, *Bioresour. Technol.* 143 (2013) 632–641.
- [33] R. Riedl, J. Dahl, I. Obernberger, M. Narodslawsky, Corrosion in fire tube boilers of biomass combustion plants, Proceedings of the China International Corrosion Control Conference, 1999, 1999.
- [34] A. Ross, K. Anastasakis, M. Kubacki, J. Jones, Investigation of the pyrolysis behaviour of brown algae before and after pre-treatment using PY-GC/MS and TGA, *J. Anal. Appl. Pyrolysis* 85 (2009) 3–10.
- [35] A.B. Ross, J.M. Jones, M.L. Kubacki, T. Bridgeman, Classification of macroalgae as fuel and its thermochemical behaviour, *Bioresour. Technol.* 99 (2008) 6494–6504.
- [36] J.S. Rowbotham, P.W. Dyer, H.C. Greenwell, M.K. Theodorou, Thermochemical processing of macroalgae: a late bloomer in the development of third-generation biofuels? *Biofuels* 3 (2012) 441–461.
- [37] P. Schiener, K. Black, M. Stanley, D. Green, The seasonal variation in the chemical composition of the kelp species *Laminaria digitata*, *Laminaria hyperborea*, *Saccharina latissima* and *Alaria esculenta*, *J. Appl. Phycol.* 27 (2015) 363–373.
- [38] J.P. Schuhmacher, F.J. Huntjens, D.W. Van Krevelen, Chemical structure and properties of coal XXVI studies on artificial coalification, *Fuel* 39 (1960) 223–234.
- [39] A.M. Smith, S. Singh, A.B. Ross, Fate of inorganic material during hydrothermal carbonisation of biomass: influence of feedstock on combustion behaviour of hydrochar, *Fuel* 169 (2016) 135–145.
- [40] M.M. Titirici, A. Thomas, S.-H. Yu, J.-O. Müller, M. Antonietti, A direct synthesis of mesoporous carbons with bicontinuous pore morphology from crude plant material by hydrothermal carbonization, *Chem. Mater.* 19 (2007) 4205–4212.
- [41] B. Wirth, J. Mumme, Anaerobic digestion of waste water from hydrothermal carbonization of corn silage, *Appl. Bioenerg.* (2014).
- [42] Q. Xu, Q. Qian, A. Quek, N. Ai, G. Zeng, J. Wang, Hydrothermal carbonization of macroalgae and the effects of experimental parameters on the properties of hydrochars, *ACS Sustainable Chem. Eng.* 1 (2013) 1092–1101.